

## DUAL-FUEL AMMONIA ENGINES TO DECARBONISE FREIGHT OPERATIONS

Abin Mathew<sup>1</sup>

Shimon Shapiro<sup>1</sup>

Xinyan Wang<sup>1</sup>

Hua Zhao<sup>1</sup>

<sup>1</sup>Centre for Advanced Powertrain and Fuels (CAPF), Brunel University of London, United Kingdom

### ABSTRACT

Operators of diesel-powered locomotives face increasing pressure to reduce carbon and exhaust emissions from their operations and transition away from using fossil fuels. Compression ignition diesel engines remain the prime movers of choice for self-powered rolling stock due to their high torque and efficiency. However, the long service life of locomotives, often exceeding 70 years, limits rapid fleet replacement. This study presents a concept for a dual-fuel diesel-ammonia internal combustion engine for locomotives, as part of ongoing research at Brunel University of London. Using data from UK Class 37 locomotives supplied by their owners and operators, representative engine duty cycles were derived from On-Train Monitoring and Recording (OTMR) data for a number of operational routes. Engine data, obtained through load bank testing of a locomotive, was then mapped onto these operational route based engine duty cycles to calculate diesel fuel use and exhaust emissions for each route. Literature based ammonia:diesel fuel ratios, validated through engine testing at Brunel University of London, were then applied to generate a comparative dual-fuel dataset. Preliminary results suggest diesel consumption - and thus carbon emissions - can be reduced by 18–29%. A CAD model was developed to demonstrate integration of ammonia fuel tanks alongside one of the two original diesel fuel tanks. Ongoing work involves using Brunel University of London's single-cylinder test engine, upgraded for ammonia fueling, to increase ammonia:diesel ratios and assess emissions impacts. The results support the potential of retrofitting existing diesel locomotives with dual-fuel capability as a transitional pathway to lower carbon rail transport.

Keywords: Ammonia, dual-fuel, decarbonization, freight operations, locomotive

### NOMENCLATURE

CBM Compressed biomethane

CNG	Compressed Natural Gas
CI	Compression ignition
ECU	Engine control unit
LBM	Liquefied biomethane
LNG	Liquefied Natural Gas
LPG	Liquefied Petroleum Gas
OTMR	On-Train Monitoring and Recording
rLPG	Renewable Liquefied Petroleum Gas

### 1. INTRODUCTION

Diesel, or compression ignition (CI), engines have long been the prime movers of choice for self-powered rolling stock, owing to their high torque and efficiency at equivalent displacement compared to spark-ignition engines. However, rising environmental concerns and increasing regulatory and public pressure in relation to exhaust emissions, air quality, carbon emissions and use of fossil fuels are all driving a shift away from fossil fuel diesel use and toward alternative cleaner propulsion technologies.

In the UK, many diesel locomotives remain in regular use well beyond their original 20-year design life, with some exceeding 70 years of service. This continued operation is driven in part by the closure of UK-based locomotive manufacturers and the country's smaller loading gauge, which requires bespoke (and thus more expensive) rolling stock designs. Locomotive designs sourced from European or North American manufacturers must be heavily modified to fit UK infrastructure, often doubling their procurement cost. Combined with a complex and costly approval process for new rolling stock, this makes fleet renewal prohibitively expensive for many operators [1,2].

Emissions regulations have also played a role. EU and UK frameworks permit the continued use of older engines so long as rebuilt units use parts equivalent to the original design. Unlike the U.S., which requires emissions upgrades during scheduled

engine rebuilds, European and UK legislation has historically imposed no such requirements. Prior to 2006, European rolling stock regulations did not apply in the UK, and while Union International de Chemins de Fer (UIC) standards existed from 2002, they were non-binding in the UK. As a result, around 90% of the UK's diesel fleet predates the first applicable emissions standard - EU Stage IIIA - and operates with no formal emissions compliance [2-10].

In this context, repowering existing locomotives with modern engines has emerged as a cost-effective alternative to full replacement. By installing new Stage V compliant engines, operators can reduce fuel consumption and emissions while avoiding the capital cost and approval burden of new rolling stock. Repowering typically costs about one-tenth of new procurement and has been successfully demonstrated in the UK on platforms such as the Class 56 and Class 73. Additionally, EU rules permit one-stage emissions derogation during repowers, allowing Stage IIIB engines in place of Stage V, further increasing practical feasibility [11-14].

Despite the lack of legislative compulsion, operators are facing increasing pressure from customers, environmental groups, and government bodies to reduce both carbon dioxide and exhaust emissions. Biodiesel and hydrotreated vegetable oil (HVO) offer "drop-in" compatibility but are more expensive than fossil diesel and provide limited improvements in non-CO<sub>2</sub> emissions. While recent trials have demonstrated the technical feasibility of fuels like HVO, the added fuel cost risks making operations economically unviable or less competitive with road freight - undermining broader modal shift goals [15]. Meaningful reductions in pollutants like particulate matter and smoke would require the integration of aftertreatment systems, yet most legacy locomotives were not designed to accommodate such equipment. Limited space and short exhaust paths restrict retrofit opportunities, and since these systems offer no operational savings, there is little financial incentive for investment.

Dual-fuel CI engines provide an attractive transition pathway. These engines operate by injecting a small amount of diesel to initiate combustion, while simultaneously introducing a second fuel - usually a gaseous fuel such as natural gas/CNG/LNG, LPG, or hydrogen - via port or direct injection. This allows use of cleaner, lower-cost fuels while preserving the high efficiency of CI combustion [16-24]. First conceptualized by Rudolf Diesel in 1901, dual-fuel technology has evolved significantly over the past century. Cooper-Bessemer Corporation began experimenting with dual-fuel CI engines in 1927, with commercial implementations by Nordberg in the 1930s and Cooper-Bessemer Corporation and the National Gas and Oil Engine Co Ltd in the 1940s [25,26]. These early systems demonstrated the improved efficiency of using gaseous fuels such as town gas and coal gas in CI mode versus spark ignition.

Today, dual-fuel engines have been deployed across rail, road, and marine sectors using fuels such as biomethane (CBM, LBM), CNG, LNG, LPG, biopropane (rLPG), methanol, and hydrogen. Recent UK projects by G-volution and SBL-Rail have applied dual-fuel technology to UK Classes 37, 59, 66, and 73, combining a Stage V diesel engine repower with dual-fuel

capability using CNG, CBM, LBM, LPG and rLPG. These locomotive concepts and the Class 73/9 dual-fuel evolution and on-network use demonstrate the practical viability of dual-fuel engines for decarbonisation of operations and emissions reduction without the need for full locomotive replacement [27,28].

In further response to this challenge, alternative carbon-free fuels have gained attention for their potential to replace conventional diesel while ensuring efficient energy utilization. Among emerging zero-carbon fuels, ammonia (NH<sub>3</sub>) has attracted increasing interest due to its high hydrogen content, global production infrastructure, and relative ease of storage and transport [29]. Unlike hydrogen, ammonia can be stored as a liquid at moderate pressure and is compatible with existing fuel logistics. It has the potential to play a major role in decarbonising combustion engines, either as a primary or secondary fuel [30].

Ammonia's combustion characteristics, however, present unique challenges. It has a high autoignition temperature (651 K), low flame speed (7–8 cm/s), and a lower heating value (18.6 MJ/kg), all of which make ignition and complete combustion more difficult in conventional CI engines [31, 32]. Early studies by Starkman et al. showed that ammonia could be used in CI engines but required modifications such as spark ignition or partial dissociation into hydrogen to improve ignition [33]. Pearsall and Garabedian explored induction methods and reported improved thermal efficiency with precise fuel control, while Sawyer et al. observed significantly elevated NO<sub>x</sub> emissions compared to hydrocarbon fuels [34, 35].

In more recent studies, Reiter and Kong demonstrated diesel-ammonia dual-fuel operation in turbocharged CI engines with up to 95% diesel replacement, achieving notable CO<sub>2</sub> reductions but variable NO<sub>x</sub> emissions depending on substitution ratio [36-38]. Gill et al. showed that partially dissociating ammonia into hydrogen improved combustion efficiency and reduced CO<sub>2</sub> emissions [39]. Niki et al. examined multiple injection strategies and ammonia fumigation, showing reductions in CO<sub>2</sub> but increases in NO<sub>x</sub> and unburned NH<sub>3</sub>, requiring careful optimization [40-43].

Kane and Northrop proposed a thermochemical recuperation system to enhance ammonia combustion, enabling higher diesel replacement but necessitating catalytic aftertreatment for unburned ammonia [44]. Scharl and Sattelmayer investigated high-pressure direct injection, finding that fuel interaction dynamics were critical for stable ignition [45]. Li et al. compared premixed charge compression ignition and gas-phase port injection strategies, both of which reduced CO<sub>2</sub> but increased hydrocarbons at low ammonia energy fractions [46]. Pei et al. demonstrated a premixed approach that improved efficiency while balancing ignition and emissions [47]. Nadimi et al. reported ammonia providing up to 84.2% of input energy, but with increased NO<sub>x</sub> and NH<sub>3</sub> emissions [48].

Recent experimental work in 2024 continues to push the envelope. Bjørgen et al. demonstrated that simultaneous high-pressure direct injection of diesel and ammonia yields improved combustion efficiency [49]. Liu et al. found that while NO<sub>x</sub> decreased at lower combustion temperatures, N<sub>2</sub>O emissions

rose significantly, highlighting the importance of aftertreatment [50]. Xiang et al. evaluated the use of diesel oxidation catalysts and selective catalytic reduction, showing NO<sub>x</sub> mitigation but challenges with N<sub>2</sub>O. Huang et al. found that optimized split injection improved combustion and reduced NO<sub>x</sub>, while Zheng et al. showed that elevated intake pressures could improve combustion but negatively affect performance under some conditions [51, 52].

These studies confirm ammonia's potential to significantly reduce CO<sub>2</sub> emissions from CI engines, especially in dual-fuel configurations. However, they also underscore the need to manage ignition stability, optimize injection strategies, and address nitrogen-based emissions such as NO<sub>x</sub>, N<sub>2</sub>O, and unburned ammonia. Emission control technologies and carefully tuned combustion strategies are essential to make ammonia viable for real-world deployment.

This work presents initial results from adopting a dual-fuel diesel-ammonia fuelling concept for the English Electric 12CSVT engine of the UK Class 37. Further work at Brunel University of London will involve additional single-cylinder engine testing to improve ammonia:diesel ratios, combustion efficiency, and emissions under varying loads. The data will inform an updated engine model and further route simulations to assess the performance and environmental impact of a UK Class 37 using improved diesel-ammonia dual-fuel engine operation.

## 2. MATERIALS AND METHODS

### 2.1 Load bank-based engine testing

Diesel-electric locomotives utilise a diesel engine to drive a generator (typically referred to as the main generator), which then supplies electrical power to traction motors located either within the vehicle frame or the bogies. Load bank testing is a method that allows the diesel engine to be evaluated under load while remaining installed in the locomotive. In this setup, the main generator is electrically isolated from the traction motors and connected instead to a resistive load bank, which simulates the electrical load normally experienced during operation. By applying load to the generator, the engine is also placed under a representative operational load.

The load bank measures the generator's current and voltage output, allowing calculation of the generator's power output using:

$$P = I \times V \quad (1)$$

Where P is the power output (in watts), I is current (in amperes), and V is voltage (in volts).

Testing was performed on a UK Class 37 locomotive in collaboration with Emission Analytics, Loram UK and Network Rail, using a locomotive owned by Network Rail and a Crestchic load bank. The procedure for disconnecting the main generator from the traction motors and interfacing with the load bank followed the guidelines provided in historical British Rail maintenance documentation [53,54]. Unlike many diesel-electric locomotives which use a notched throttle control, the UK Class 37 features a continuously variable power lever. The driver can position the lever anywhere between idle and full power, with

the lever's position directly controlling the engine output. The lever communicates the power demand via a pneumatic signal ranging from 0 to 310 kPa which is transmitted to the engine governor. For power lever positions between 0° and 40° from the idle stop (corresponding to a pneumatic signal of 0–140 kPa), the engine governor reduces engine speed from the idle value of 460 rpm whilst also increasing fuel supply and therefore also increasing engine power. Between 40° and 90° lever angles (140–310 kPa signal range), the governor increases both engine speed and fuel delivery, allowing the engine to reach a maximum speed of 890 rpm at full power.

The pneumatic signal was measured using a Druck DPI 705 digital pressure gauge connected, via an adaptation fitting to the locomotive's 'rail air' connector. This is located above the buffers at the front of the locomotive and is used to share regulator air signals between two locomotives operating in multiple.

### 2.2 Fuel Consumption Measurement and Exhaust Emissions Measurement

Fuel consumption was measured using a temporary fuel tank inserted into the locomotive's fuel supply and return lines in place of the original tank. A 250-litre, 45° cone-bottom polyethylene tank (supplied by Tanks UK) was mounted in a steel frame and placed on an Adam Equipment CPW 200L scale. The scale, with a maximum capacity of 200 kg and an accuracy of ±0.05 kg (±0.025% full scale), recorded mass data via an RS232 serial connection at 1 Hz using Adam Equipment's DU software and a Windows laptop. The measurement duration at each engine operating point was adjusted to ensure that the recorded mass change was accurate to within 1%.

Exhaust emissions were measured in collaboration with Emissions Analytics. Gaseous emissions - including carbon monoxide (CO), carbon dioxide (CO<sub>2</sub>), nitric oxide (NO), nitrogen dioxide (NO<sub>2</sub>), total hydrocarbons (THC) and oxygen (O<sub>2</sub>) - were analyzed using a SEMTECH LDV system comprising the SEMTECH GAS, SCS, and EFM4 modules. Particulate emissions - both total particulate mass (PM) and total particulate number (PN) - were measured using a Pegasor Mi2. Exhaust sample lines were inserted into the exhaust outlet of one of the two turbochargers on the English Electric 12CSVT engine fitted to the UK Class 37 locomotive. This is a V12 with one turbocharger per bank and a separate exhaust outlet for each. The exhaust exits via a short, unsilenced pipe through the locomotive roof, with no aftertreatment systems installed between the turbocharger outlet and exhaust exit.

### 2.3 Exhaust Mass Flow Rate Calculation

Due to space constraints ahead of the air intake and the absence of suitably long or wide intake ducts to condition airflow, it was not possible to measure engine air mass flow rate directly. As a result, exhaust mass flow rate was calculated using the method specified in the European Union's Non-Road Mobile Machinery (NRMM) regulations, which outline general testing procedures and emission limits for engines used in non-road applications, including railway vehicles [8].

Exhaust mass flow from fuel mass flow rate.

$$q_{mew,i} = q_{mf,i} \cdot \left[ \frac{1.4 \cdot w_c^2}{(1.0828 \cdot w_c + k_{fd} \cdot f_c)} \right] \left( \frac{H_a}{1000} \right) + 1 \quad (2)$$

$$f_c = 0.5411 \cdot (C_{CO2,d} - C_{CO2,a}) + \frac{C_{COd}}{18522} + \frac{C_{HCw}}{17355} \quad (3)$$

Where:

$q_{mew,i}$  = wet exhaust gas mass flow rate (kg/s)

$q_{mf,i}$  = instantaneous fuel mass flow rate (kg/s)

$w_c$  = carbon content of fuel (% mass)

$H_a$  = intake air humidity (g H<sub>2</sub>O/kg dry air), equivalent to ambient humidity

$k_{fd}$  = combustion additional volume on a dry basis (m<sup>3</sup>/kg fuel)

$f_c$  = carbon factor

$C_{CO2,d}$  = dry CO<sub>2</sub> concentration in the exhaust gas (%)

$C_{CO2,a}$  = dry CO<sub>2</sub> concentration in the ambient air (%)

$C_{COd}$  = dry CO concentration in the exhaust gas (ppm)

$C_{HCw}$  = wet HC concentration in the exhaust gas (ppm)

$$k_{fd} = k_f - 0.11118 \cdot w_H \quad (4)$$

Where:

$k_f$  = fuel specific factor (as below)

$w_H$  = hydrogen content of the fuel (% mass)

$$k_f = 0.055594 \cdot w_H + 0.0080021 \cdot w_N + 0.0070046 \cdot w_O \quad (5)$$

Where:

$w_H$  = hydrogen content of the fuel (% mass)

$w_N$  = nitrogen content of the fuel (% mass)

$w_O$  = oxygen content of the fuel (% mass)

Ambient humidity was measured by the SEMTECH LDV and a sample of the fuel was analysed by Coryton Fuels to provide the elemental mass values per unit mass of the fuel.

## 2.4 Mass flow rate calculations for gaseous exhaust species and PM and number flow rate calculations for PN

Following the calculation of exhaust mass flow rate per engine test point the following was used to calculate the mass flow rate of each gaseous species in the exhaust. Whilst exhaust emissions concentrations (for gaseous species) or mass per unit volume (for PM) or number per unit volume (for PN) were measured from only one of the two engine banks and one of the two exhaust pipes this does not need to be accounted for in these calculations since the engine's overall fuel mass flow rate was measured and it was assumed the fuel consumption and emissions were equal for each of the two banks of the V12 engine.

$$q_{mgas,i} = k_h \cdot k \cdot u_{gas} \cdot q_{mew,i} \cdot c_{gas,i} \cdot 3600 \quad (6)$$

Where:

$q_{mgas,i}$  = emission rate of a gaseous species in g/h

$k_h$  = NO<sub>x</sub> correction factor (based on ambient humidity)

$k = 1$  for  $c_{gas,i}$  in ppm or  $k = 10,000$  for  $c_{gas,i}$  in % volume

$u_{gas}$  = component specific factor (see table)

$q_{mew,i}$  = exhaust gas mass flow rate (kg/s)

$c_{gas,i}$  = emission concentration in the raw exhaust gas in ppm or % volume

$$k_h = \frac{15.698 \cdot H_a}{1000} + 0.832 \quad (7)$$

$H_a$  = humidity of intake air, equivalent to ambient humidity (g H<sub>2</sub>O / kg dry air)

Gas	NO <sub>x</sub>	CO	HC	CO <sub>2</sub>	O <sub>2</sub>	CH <sub>4</sub>
$u_{gas}$	0.001586	0.000966	0.000482	0.001517	0.001103	0.000553

For PM and PN measurements the Pegasor Mi2 provides measurements for PM in mg/m<sup>3</sup> and for PN in number of particles per cm<sup>3</sup>.

The following was used to convert to PM and PN measurements to mg/hr and number per hour respectively.

$$\text{PM (mg/hr)} = [\text{PM measurement (mg/m}^3\text{)} \cdot \text{exhaust mass flow rate (kg/hr)}] / 1.29 \text{ kg/m}^3 \quad (8)$$

$$\text{PN (Number per hours)} = [\text{PN measurement number per cm}^3 \cdot \text{exhaust mass flow rate (kg/hr)}] / 1.29 \quad (9)$$

## 2.5 Load bank engine test procedure

The load bank measures the voltage and current of the main generator and so, as above, the main generator's power can be calculated. However, as per Figure 1, the overall engine power output includes power delivered to the auxiliary generator for auxiliary loads and the mechanical load of the hydraulic connection between the crankshaft and the cooling fan.

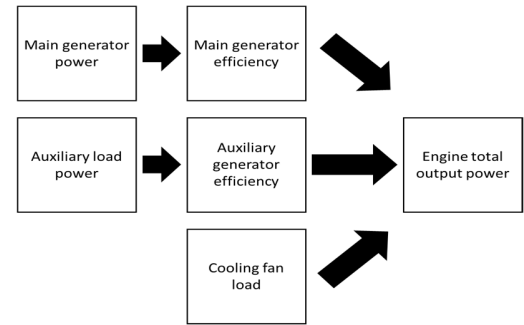


**FIGURE 1: CONTRIBUTIONS TO TOTAL ENGINE POWER OUTPUT FOR A UK CLASS 37 LOCOMOTIVE**

The load bank was also used to measure the output of the auxiliary generator. This auxiliary generator powers electric motors for the air compressors, traction motor blower motors, fuel pump and also powers the cab desk, electronic control, signalling systems, lighting, and heating of the locomotive. The specifications of these items were noted from [54] but further verified (due to potential changes in component specifications since original build) by powering these items incrementally by the locomotive's on-board batteries and noting both the voltage and current draw of the auxiliary system. The maximum

auxiliary load was noted as 32kW and the load of the mechanical and hydraulic connection between the engine's crankshaft and the cooling fans was noted from British Rail documents as 39.5 kW. During the locomotive's in-service operation, the auxiliary loads for the fuel pump, traction motor blower motors, cab desk, electronic control systems and signalling systems are constant whereas the air compressors, lighting, heating and mechanical-hydraulic drive for the cooling fans are all intermittent. For the load bank testing the air compressors were isolated by supplying the locomotive with a compressed air supply from the depot's shop air, thus topping up the air tanks as required without activating the locomotive's air compressors. Lighting and heating systems were switched off. The mechanical-hydraulic connection between the engine's crankshaft and the cooling fans featured an electronic clutch which alongside the cooling system's thermostat controls the temperature of the engine coolant. The switch features an override function and this was engaged for all of the load bank testing i.e. the cooling fans ran continuously. The thermostat of the cooling system being relied up to avoid overcooling of the engine. Engine coolant temperature was measured by a K-type thermocouple placed at the exit of the coolant from the engine and ahead of the radiator cooling circuit.

As the UK Class 37 has a non-notched driver power lever and thus a non-notched operation of the engine's power output, the engine was tested at 10 points from idle to maximum power. At each operating point the engine was allowed to stabilise for 2 minutes prior to data being recorded.

The initial results of regulator air pressure versus main generator output were processed to calculate the engine's total power output by first considering the main generator's efficiency of 93% and the auxiliary generators output and its efficiency of 85% [54]. With all other auxiliary loads stabilised and the mechanical load of the hydraulic connection to drive the cooling fans also known, the engine's total power output per operating point was calculated. Fuel consumption and exhaust emissions data was then referenced to the engine's total power output for each of the engine operating points.

## 2.6 OTMR based route simulations

On-train monitoring and recording systems (OTMR) are mandatory for UK locomotives and are effectively the equivalent of "black boxes" for aircraft. RIS-2472-RST details the requirements for OTMR for UK locomotives [55]. The minimum requirement for the driver's power demand channel is simply if power is on or off i.e. at or away from the idle position. However, some OTMR system suppliers log additional information e.g. the air pressure signal from the driver's power lever to the engine governor or the main generator voltage and current.

OTMR data were provided for a number of UK Class 37 operations by Colas Rail Freight. The QTron system used for the OTMR data of this work logged a number of additional parameters beyond the minimum required of UK OTMR systems and this included both the air pressure signal from the driver's power lever as well as main generator voltage and current. Using a look up table of regulator air pressure versus main generator

power noted from load bank testing allowed the OTMR data of a route to be converted into main generator power output over time for each route. Alternatively, a direct use of the main generator voltage and current data from the OTMR data provided a main generator output power over time for each route. By correcting this data for main generator efficiency, adding auxiliary load and correcting for auxiliary generator efficiency meant an engine duty cycle for total engine power over time could be developed for each route. Total engine power was then used as the input to look up tables of fuel consumption (in g/s) and exhaust emissions (in g/s for gaseous emissions, mg/s for PM and number/s for PN) to give instantaneous, cumulative and total fuel consumption and exhaust emissions for the original English Electric 12CSV engine. With this approach the route models can be re-run considering different auxiliary loads or applied to a new engine used in a proposed repower. In the first instance auxiliary load in the route simulations was fixed for the non-intermittent auxiliary loads of the engine's fuel pump, traction motor blower motors, cab desk, electronic control systems and signalling systems. Lighting, heating and intermittent air compressors were not included and the radiator fan was set to operate continuously. Future work will consider addition of heating, lighting and intermittent air compressors and radiator cooling fans.

To assess the impact of evolving the UK Class 37's English Electric 12CSV engine to a dual-fuel diesel-ammonia our initial work completed a literature review to understand the indicative ammonia:diesel ratios that could be achieved with stable combustion versus increasing engine load. These were later validated using the single-cylinder HD engine at Brunel University of London. By applying these ammonia:diesel ratios to the original load bank-based data provided a comparative dataset of diesel and ammonia fuel consumption for the proposed dual-fuel engine. This data was then mapped as above to the same OTMR based engine duty cycles to once again provide an instantaneous, cumulative and total diesel and ammonia fuel consumption for each route. Thus, giving a direct comparison of the original diesel engine with the evolved diesel-ammonia dual-fuel engine.

## 2.7 Dual-fuel diesel-ammonia single-cylinder setup at CAPF

The experimental engine studies were carried out on a 2-litre single-cylinder heavy duty diesel engine. Detailed engine specifications are depicted in Table 1. The load is applied using an absorption type eddy current dynamometer and the heat generated during engine loading is removed by external cooling water. An electrical starter motor coupled to the dynamometer is used to start the engine. Intake air to the engine was either supplied by natural aspiration or using an external compressor and was measured using a thermal mass flow meter. Two surge tanks were installed in each of the intake and exhaust lines to mitigate pressure oscillations. Additionally, an exhaust throttle was used to simulate turbocharger back pressure at 0.10 bar above intake manifold pressure. Furthermore, engine coolant and lubrication oil were supplied by external pumps and

temperatures of oil, water, intake air and EGR were controlled by heaters and water-cooled heat exchangers.

**TABLE 1: ENGINE SPECIFICATIONS**

Parameter	Value
Displaced volume	2026 cm <sup>3</sup>
Compression ratio	16.8
Bore x stroke	129 x 155 mm
Connecting rod length	256 mm
Maximum in-cylinder pressure	18 MPa
Piston type	Stepped-lip bowl
Number of valves	4
Exhaust valve timing	EVO 144° & EVC 360° ATDC
Inlet valve timing	IVO 366° & IVC 531° ATDC

## 2.8 Fuel Properties and Delivery

In this work liquid ammonia was supplied via port fuel injection using the system shown in Figure 2. Pilot fuel diesel was supplied by direct injection. Four ammonia cylinders with full length dip tubes were used and to avoid vaporization, an air driven ammonia pump was used to pressurize ammonia up to 40 bar. A pulsation damper was used to regularize flow and to damp pressure fluctuations. A prototype PFI ammonia injector, controlled by a G-volution ECU, was used to supply liquid ammonia into the intake manifold close to the intake valves. An automatic shutdown system using a solenoid valve was included to ensure safety. The diesel supply system consisted of a common rail system which supplied diesel at a pressure between 50–240 MPa via an 8-hole Bosch diesel injector (CRIN3-22 0446B00482) which could deliver up to 3 injections per cycle. The engine speed governor function of an ECE ECU adjusted the mg/stroke injection and thus the diesel flow rate to maintain the engine speed requested by the user. Coriolis flow meters were used to measure the quantity of ammonia and diesel supplied to engine.

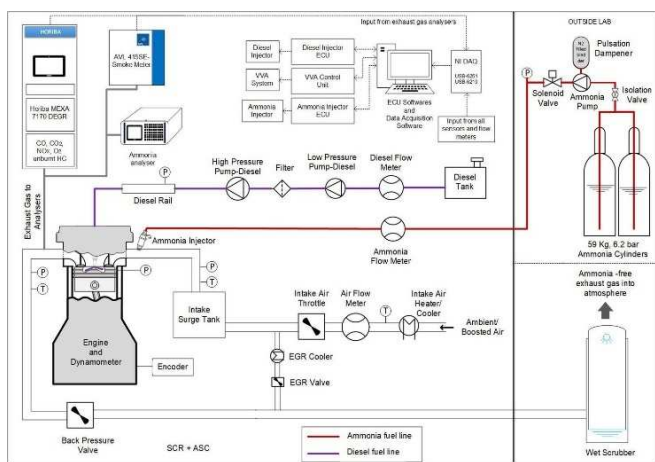


**FIGURE 2: SCHEMATIC OF THE EXPERIMENTAL SETUP**

## 2.9 Exhaust gas measurement and exhaust gas scrubber for mitigating ammonia

All regulated exhaust emissions were measured using standard, well-established techniques. Gaseous emissions - including carbon monoxide (CO), carbon dioxide (CO<sub>2</sub>), nitrogen oxides (NO<sub>x</sub>), total hydrocarbons (THC), and oxygen (O<sub>2</sub>) - were measured using a Horiba MEXA-7170 DEGR emissions analyzer. CO and CO<sub>2</sub> were quantified using non-dispersive infrared (NDIR) spectroscopy, while NO<sub>x</sub> was measured via the chemiluminescence method. Hydrocarbons were detected using a flame ionization detector (FID), and oxygen concentration was determined using a magneto-pneumatic (MPA) detector. Prior to each engine test, the emissions analyzer was calibrated using certified span gases to ensure measurement accuracy and linearity. A high-pressure sampling module enabled gas extraction upstream of the exhaust back pressure valve and a heated sampling line maintained the gas temperature at approximately 464 K to prevent condensation. Particulate emissions were measured using an AVL 415SE smoke meter. A sampling time of 30 seconds was used to draw exhaust gas through a filter paper, with smoke quantified in terms of Filter Smoke Number (FSN). Ammonia (NH<sub>3</sub>) emissions were measured using a Signal Nebula S4, a Tunable Diode Laser Spectroscopy (TDLS) based analyzer, selected for its fast response and high measurement accuracy. Analog signals (0–10 V) from all analyzers were acquired using a National Instruments USB-6210 DAQ card. By first summing the air mass flow rate and fuel mass flow rates to calculate the exhaust mass flow rate, equations (6) and (7) were then used to calculate the mass flow rate of each gaseous emission species.

A bespoke wet scrubber, using water as the scrubbing medium, was installed downstream of the emission measurement system to treat the exhaust gases before their release into the atmosphere. The scrubbing water reacted with ammonia to form ammonium hydroxide and the resulting solution was collected and disposed of following laboratory hazardous waste management protocols.

## 2.10 Data Acquisition and Control

Two National Instruments data acquisition (DAQ) systems were employed to monitor engine operation and capture real-time experimental data. A USB-6353 high-speed DAQ card was used to record crank-angle resolved data, synchronized with an EB58 optical encoder offering a resolution of 0.25° crank angle (CA). Simultaneously, a USB-6218 DAQ card handled low-frequency measurements, including pressures, temperatures, and flow rates across the fuel and intake/exhaust systems.

In-cylinder pressure was measured using a Kistler 6125C11 piezoelectric sensor, coupled with an AVL FI Piezo amplifier, delivering a sensitivity of 33.53 pC/bar and a measurement range of 0–300 bar (rated up to 200 bar at 250 °C). The amplifier's cyclic drift compensation feature eliminated the need for zeroing and maintained amplitude/phase accuracy. A 100 kHz filter was applied to minimize phase errors. Top Dead Center (TDC) referencing and synchronization were achieved using the EB58 encoder, while intake and exhaust manifold pressures were recorded using Kistler 4049A10S and 4049A10SP22 sensors (0–10 bar, ±0.5% FS accuracy). Valve lift measurements for the

Variable Valve Actuation (VVA) system were recorded using a LORD MicroStrain S-DVRT-8 displacement sensor with a 0–24 mm range,  $\pm 1.0\%$  accuracy, and  $\pm 1.0 \mu\text{m}$  repeatability. Valve timing events (IVO/IVC) were defined at 0.5 mm lift, using signal data post-processed with a 0.56 ms delay to correct phase offset at 1200 rpm. Diesel injection timing was determined using a LEM PR30 current probe (0–20 A,  $\pm 1\%$  accuracy), capturing injector control signals from the ECE ECU. Diesel injection pressure was monitored using a Bosch DS-HD-RDS4.5 high-pressure transducer (0–2400 bar,  $\pm 0.7\text{--}1.7\%$  FS). Engine speed was measured via a Texcel V4 controller (Froude dynamometer system), accurate to  $\pm 1$  rpm over 0–8000 rpm, while brake torque was obtained using a Froude Hofmann AG150 eddy current dynamometer (0–500 Nm,  $\pm 0.25\%$  FS accuracy,  $\pm 0.15\%$  FS repeatability).

Oil pressure was measured using GE PMP 5076 (0–10 bar,  $\pm 0.2\%$  FS). Ammonia flow was monitored using an Endress+Hauser Promass 80A02 Coriolis flow meter (0–20 kg/h,  $\pm 0.15\%$  accuracy,  $\pm 0.05\%$  repeatability). Diesel fuel flow was determined by measuring both supply and return lines using Endress+Hauser Promass 83A01 (0–100 kg/h) and 83A02 (0–20 kg/h) respectively, each with  $\pm 0.10\%$  accuracy and  $\pm 0.05\%$  repeatability. Air flow was captured via an Endress+Hauser T-mass 65F thermal mass flow meter (0–910 kg/h,  $\pm 1.5\%$  accuracy,  $\pm 0.5\%$  repeatability). Temperatures (intake, exhaust, coolant, EGR and oil) were measured using Audon TCK-4 thermocouple amplifiers and K-type thermocouples, supporting a range of  $-40^\circ\text{C}$  to  $1200^\circ\text{C}$ , with an accuracy of  $\pm 2.5^\circ\text{C}$  or  $\pm 0.75\%$  of the reading.

All signals were logged using a LabVIEW based software developed in-house, which displayed measurements live and stored them in 300-cycle intervals for post-processing. Crank-angle resolved data acquired through the high-speed USB-6353 DAQ system was processed using the Viatech Combustion Analysis Toolkit (VCAT), a specialized software platform for real-time in-cylinder pressure measurement and combustion analysis. VCAT is compatible with National Instruments DAQ hardware and enables synchronized, cycle-by-cycle evaluation of key combustion parameters.

### 3. RESULTS AND DISCUSSION

#### 3.1 Locomotive load bank testing and test cell results

Figure 3 summarizes the main generator power and corrected total engine power versus the regulator air pressure / driver's power lever signal sent to the engine governor. This also shows, as per British Rail documentation, that the engine speed is allowed to initially fall as the engine begins to generate power, thereafter rising with increasing power outputs. Fuel consumption and exhaust emissions data were referenced to total engine power and regulator air pressure for use in look up tables in OTMR based route simulations as detailed above. These datasets are not included in this work, however general trends are shown in Figure 4.

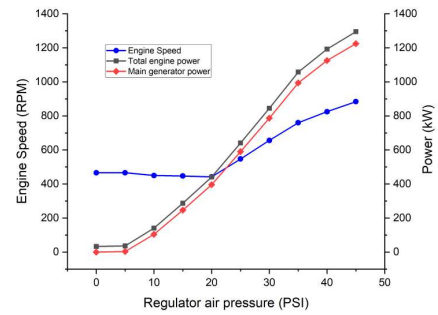


**FIGURE 3:** LOAD BANK RESULTS FOR REGULATOR AIR PRESSURE VERSUS MAIN GENERATOR AND TOTAL ENGINE POWER

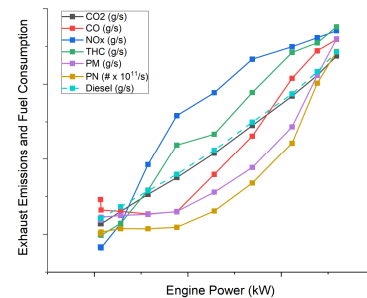


**FIGURE 4:** FUEL CONSUMPTION AND EMISSION TRENDS FROM LOAD BANK TESTING

Figure 5 summarizes the literature review-based ammonia:diesel ratios, later validated by testing using the single-cylinder HD engine at CAPF, that can be reliably achieved versus engine load. This data was applied to the load bank derived fuel consumption versus total engine power dataset to provide a comparative dual-fuel engine dataset which was then used in a look up table and mapped onto OTMR based route simulations. Thus, giving a direct comparison of the original and dual-fuel evolved engine.

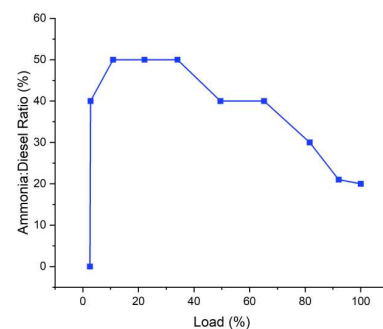


**FIGURE 5:** AMMONIA:DIESEL RATIOS USED IN THE ROUTE SIMULATIONS OF THIS WORK

Pressure-crank angle data for various ammonia:diesel ratios is shown in Figure 6 (1200 rpm, 3 bar IMEP). As the ammonia energy contribution in the fuel increased, the onset of combustion was delayed and the combustion duration was longer

than for diesel alone owing to the poor combustion characteristics of ammonia.

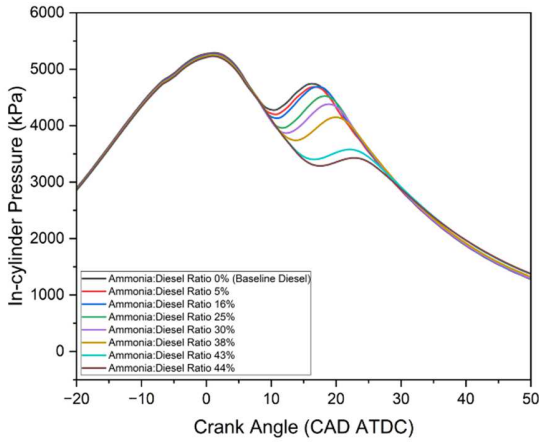


**FIGURE 6:** PRESSURE-CRANKANGLE DIAGRAM FROM DIESEL-AMMONIA DUAL-FUEL STUDIES

### 3.2 UK Class 37 equipment layout, CAD model and route simulation results

Figure 7 shows the equipment layout for a UK Class 37 locomotive (following refurbishment in the 1980s) and our proposal for replacing one of the two diesel fuel tanks with two 1000 liter ammonia fuel tanks.

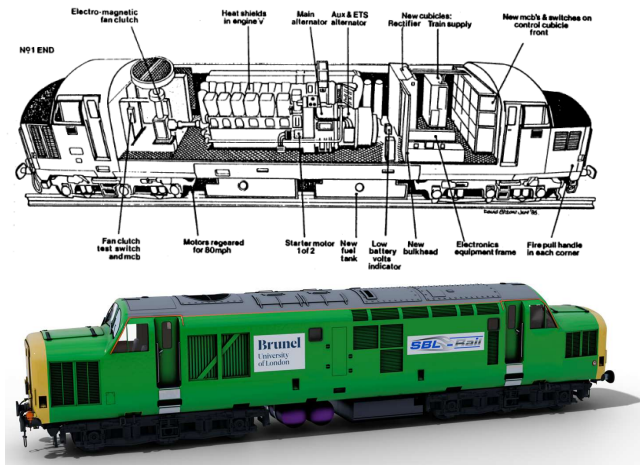


**FIGURE 7:** EQUIPMENT LAYOUT AND CAD MODEL

Route simulation results referred to as ‘full data’ use all the OTMR data for a day’s operation including idling prior to and at the end of a route. ‘Section’ refers to just the portion of OTMR data for once the locomotive is travelling along a route. These results show the significant future scope for using dual-fuel combustion during engine idling too and following further combustion optimization and development work.

The results show how diesel fuel consumption and thus carbon emissions can be reduced by up to 29% using a dual-fuel

engine which uses a maximum ammonia:diesel ratio of 50:50 and with a 20:80 ratio at full load.

**TABLE 2:** SUMMARY OF DIESEL AND DUAL-FUEL ENGINE FUEL CONSUMPTION FROM ROUTE SIMULATIONS

Route number	% diesel reduction	
	Full data	Section
1	17.4	29.1
2	14.3	27.5
3	17.0	18.4
4	10.3	20.3

### 4. CONCLUSION

This work shows the positive impact of adopting a dual-fuel diesel-ammonia engine for locomotive operations and a proposal for packaging ammonia fuel tanks in place of part of the diesel fuel storage tanks. By adopting a dual-fuel engine, operators can reduce carbon emissions by up to 29%. With further development and optimization of dual-fuel diesel-ammonia combustion underway there is significant scope to further reduce diesel fuel use and provide a transitional pathway to decarbonize existing internal combustion engine powered locomotives.

### ACKNOWLEDGEMENTS

We would like to express our appreciation to our project partners Coryton Fuels, Colas Rail Freight, Eminox, Emission Analytics, G-volution, Loram UK, Network Rail, and SBL-Rail for their support and assistance with this work.

### REFERENCES

- [1] Pritchard, Robert. British Railways Locomotives and Rolling Stock. Platform 5, Sheffield, (2024).
- [2] Shapiro, Shimon. “Dual-Fuel Evolution and Repower of the Class 37 Locomotive.” MRes Thesis. University of Birmingham, Birmingham, United Kingdom. 2023.
- [3] G-volution, “RSSB Future Railway Competition, Phase 1 submission report, project reference 104 POT 04.” G-volution, Bristol, United Kingdom. 2016.
- [4] Agarwal, Avinash., Dhar, Atul., Gautam, Anirudh, and Pandey, Ashok. *Locomotives and Rail Road Transportation: Technology, Challenges and Prospects*. Springer, Berlin (2017).
- [5] Shapiro, Shimon. “Review of the exhaust emissions legislative landscape for railway vehicles pre-EU Stage IIIA.” SBL-Rail, Manchester. United Kingdom. 2018.
- [6] Shapiro, Shimon and Smith, Chris. “Review of EU and US emissions regulations for railway vehicles.” G-volution, Bristol. United Kingdom. 2018.
- [7] Shapiro, Shimon. “The UK’s autonomously powered passenger vehicle rail fleet and the opportunity to adopt dual-fuel

engines.” University of Birmingham, Birmingham, United Kingdom. 2018.

[8] “European Union Non-Road Mobile Machinery, 19.12.2016 C(2016) 8381 final, Annex 7, Commission Delegated Regulation (EU) supplementing Regulation (EU) 2016/1628 of the European Parliament and of the Council with regard to technical and general requirements.” Brussels, Belgium. 2018.

[9] “Stage V non-road emission standards.” ICCT, Berlin, Germany. 2016.

[10] “Control of Emissions from Locomotives.” Title 40, Chapter I, Subchapter U, Part-1033. Environmental Protection Agency. Washington, District of Columbia. 2024.

[11] Clinnick, Richard. “Built in the 1960s... rebuilt for the 21st century.” Rail, Bauer Consumer Media Ltd. Peterborough. 2014.

[12] Foster, Stefanie. “First GB Railfreight rebuilt '73/9' on test at Loughborough. Rail, Bauer Consumer Media. Peterborough. 2014.

[13] Foster, Stefanie. “RVEL unveils re-engineered Ultra73 for Network Rail”. Rail, Bauer Consumer Media. Peterborough. 2014. RVEL unveils re-engineered Ultra73 for Network Rail

[14] Clinnick, Richard. “The GB Railfreight Class 69 project explained”. Rail, Bauer Consumer Media. Peterborough. 2020.

[15] “DB Cargo UK tests hydrotreated vegetable oil locomotive fuel”. Railway Gazette International. DVV Media International Ltd. London. 2020.

[16] Karim. “The Dual-Fuel Engine of the compression ignition type.” *SAE Technical Paper* 831073 (1983).

[17] Heenan and Geetel. “Dual-Fueling Diesel/NGV Technology.” *SAE Technical Paper* 881655 (1988).

[18] Hountalas and Papaglannakis. “Theoretical and experimental investigation of a direct injection dual-fuel diesel-natural gas engine.” *SAE Technical Paper* 2002-01-0868 (2002).

[19] Suzuki and Tsujimura. “The combustion improvements of hydrogen/diesel dual-fuel engine”. *SAE Technical Paper* 2015-01-1939 (2015).

[20] “Low carbon truck and refuelling infrastructure demonstration trial evaluation - final report to the DfT”. Cenex, Loughborough, United Kingdom. 2016.

[21] Mustafi, Nirendra, Raine and Bryony. “Characterisation of exhaust particulates from a dual fuel engine” *Aerosol science and technology*, pp. 954-963.

[22] Smith, Kevin. “LNG: fuel of the future?”. *International Railway Journal*. Simmons-Boardman Publishing Corporation, Omaha, Nebraska. 2013.

[23] Pirouzpaneh, Mohammadi, Barkhordarion, “Dual-fuelling of an industrial indirect injection diesel engine by diesel and LPG.” *International Journal of Energy Research*, pp903-912 , 1996.

[24] Weaver and Turner. “Dual fuel natural gas/diesel engines: technology, performance and emissions.” *SAE Technical Paper* 940548 (1994).

[25] Diesel, Rudolf. “Method of igniting and regulating combustion for internal-combustion engines.” US, Patent No. US673160A.1901.

[26] Boyer. “Status of dual fuel engine development.”. *SAE Journal* May (1949)

[27] Shapiro, Shimon. “Development and demonstration of dual-fuel diesel & bioLPG/rLPG locomotives”. WLPGA LPG Week, Global Technology Conference, New Delhi, India. 2002.

[28] “Dual fuel concepts revealed”. Rail Director. Rail Business Daily, Leeds, United Kingdom. 2022.

[29] Herbinet, Olivier, Bartocci, Patrizia, and Grinberg Dana, Ariel. “On the Use of Ammonia as a Fuel – A Perspective.” *Fuel Communications* VOL. 11 No. 1 (2022): pp. 100064. DOI: 10.1016/j.fueco.2022.100064.

[30] Kurien, Caneon, and Mittal, Mayank. “Utilization of Green Ammonia as a Hydrogen Energy Carrier for Decarbonization in Spark Ignition Engines.” *International Journal of Hydrogen Energy* VOL. 48 No. 74 (2023): pp. 28803–28823. DOI: 10.1016/j.ijhydene.2023.04.073.

[31] Shah, Zubair Ali, Mehdi, Ghazanfar, and Congedo, Paolo Maria. “A Review of Recent Studies and Emerging Trends in Plasma-Assisted Combustion of Ammonia as an Effective Hydrogen Carrier.” *International Journal of Hydrogen Energy* VOL. 51 No. 1 (2024): pp. 354–377. DOI: 10.1016/j.ijhydene.2023.05.222.osti.gov

[32] Xu, Xiaowei, Liu, Enlong, and Zhu, Neng. “Review of the Current Status of Ammonia-Blended Hydrogen Fuel Engine Development.” *Energies* VOL. 15 No. 3 (2022): pp. 1023. DOI: 10.3390/en15031023.

[33] Starkman, Eugene S., James, George E., and Newhall, Harold K. “Ammonia as a Diesel Engine Fuel: Theory and Application.” *SAE Technical Paper* VOL. 670946 No. 1 (1966): pp. 1–20. DOI: 10.4271/670946.

[34] Pearsall, Thomas J., and Garabedian, Charles G. “Combustion of Anhydrous Ammonia in Diesel Engines.” *SAE*

*Technical Paper* VOL. 670947 No. 1 (1967): pp. 1–9. DOI: 10.4271/670947.

[35] Sawyer, Richard F., Starkman, Eugene S., Muzio, Louis, and Schmidt, William L. “Oxides of Nitrogen in the Combustion Products of an Ammonia Fueled Reciprocating Engine.” *SAE Technical Paper* VOL. 680401 No. 1 (1968): pp. 1–12. DOI: 10.4271/680401.

[36] Reiter, Adam J., and Kong, Song-Chang. “Combustion and Emissions Characteristics of Compression-Ignition Engine Using Dual Ammonia-Diesel Fuel.” *Fuel* VOL. 90 No. 1 (2011): pp. 87–97. DOI: 10.1016/j.fuel.2010.07.055.

[37] Reiter, Adam J., and Kong, Song-Chang. “Diesel Engine Operation Using Ammonia as a Carbon-Free Fuel.” *Proceedings of the ASME Internal Combustion Engine Division Fall Technical Conference* VOL. 2010 No. 1 (2010): pp. 111–117. DOI: 10.1115/ICEF2010-35026.

[38] Reiter, Adam J., and Kong, Song-Chang. “Demonstration of Compression-Ignition Engine Combustion Using Ammonia in Reducing Greenhouse Gas Emissions.” *Energy & Fuels* VOL. 22 No. 5 (2008): pp. 2963–2971. DOI: 10.1021/ef800140f.

[39] Gill, Sarbjit S., Chatha, Gurcharn S., and Tsolakis, Andreas. “Assessing the Effects of Partially Decarbonising a Diesel Engine by Co-Fuelling With Dissociated Ammonia.” *International Journal of Hydrogen Energy* VOL. 37 No. 7 (2012): pp. 6074–6083. DOI: 10.1016/j.ijhydene.2011.12.137.

[40] Niki, Yusuke, Yoo, Donghoon, and Hirata, Katsuhiko. “Effects of Ammonia Gas Mixed Into Intake Air on Combustion and Emissions Characteristics in Diesel Engine.” *SAE Technical Paper* VOL. 2022-01-0923 No. 1 (2022): pp. 1–9. DOI: 10.4271/2022-01-0923.

[41] Niki, Yusuke, Nitta, Yusuke, and Sekiguchi, Hiroshi. “Emission and Combustion Characteristics of Diesel Engine Fumigated With Ammonia.” *SAE Technical Paper* VOL. 2022-01-0931 No. 1 (2022): pp. 1–8. DOI: 10.4271/2022-01-0931.

[42] Niki, Yusuke, Nitta, Yusuke, and Sekiguchi, Hiroshi. “Diesel Fuel Multiple Injection Effects on Emission Characteristics of Diesel Engine Mixed Ammonia Gas Into Intake Air.” *SAE Technical Paper* VOL. 2022-01-0935 No. 1 (2022): pp. 1–10. DOI: 10.4271/2022-01-0935.

[43] Niki, Yusuke. “Experimental Investigation of Effects of Split Diesel-Pilot Injection on Emissions from Ammonia-Diesel Dual Fuel Engine.” *ASME Internal Combustion Engine Division Fall Technical Conference* VOL. 2021 No. 1 (2021): pp. V001T01A002. DOI: 10.1115/ICEF2021-65512.

[44] Kane, Steven P., and Northrop, William F. “Thermochemical Recuperation to Enable Efficient Ammonia-Diesel Dual-Fuel Combustion in a Compression Ignition

Engine.” *Energies* VOL. 14 No. 22 (2021): pp. 7540. DOI: 10.3390/en14227540.

[45] Scharl, Valentin, and Sattelmayer, Thomas. “Ignition and Combustion Characteristics of Diesel Piloted Ammonia Injections.” *Fuel Communications* VOL. 11 No. 1 (2022): pp. 100068. DOI: 10.1016/j.jfueco.2022.100068.

[46] Li, Tianxin, Duan, Yujing, and Wang, Yanjun. “Research Progress of Ammonia Combustion Toward Low Carbon Energy.” *Fuel Processing Technology* VOL. 248 No. 1 (2023): pp. 107821. DOI: 10.1016/j.fuproc.2023.107821.

[47] Pei, Yiqiang, Wang, Decheng, and Jin, Shouying. “A Quantitative Study on the Combustion and Emission Characteristics of an Ammonia-Diesel Dual-Fuel (ADDF) Engine.” *Fuel Processing Technology* VOL. 250 No. 1 (2023): pp. 107906. DOI: 10.1016/j.fuproc.2023.107906.

[48] Nadimi, Ehsan, Przybyła, Grzegorz, and Lewandowski, Mariusz T. “Effects of Ammonia on Combustion, Emissions, and Performance of the Ammonia/Diesel Dual-Fuel Compression Ignition Engine.” *Journal of the Energy Institute* VOL. 107 No. 1 (2022): pp. 206–216. DOI: 10.1016/j.joei.2022.10.006.

[49] Bjørgen, Karl Oskar Pires, Emberson, Daniel R., and Løvås, Terese. “Combustion of Liquid Ammonia and Diesel in a Compression Ignition Engine Operated in High-Pressure Dual Fuel Mode.” *Fuel* VOL. 360 No. 1 (2024): pp. 128269. DOI: 10.1016/j.fuel.2024.128269.

[50] Liu, Jian, and Liu, Jun. “Experimental Investigation of the Effect of Ammonia Substitution Ratio on an Ammonia-Diesel Dual-Fuel Engine Performance.” *Journal of Cleaner Production* VOL. 434 No. 1 (2023): pp. 140274. DOI: 10.1016/j.jclepro.2023.140274.

[51] Huang, Liang, Zheng, Lei, and Zhang, Rui. “Experimental Study on Combustion and Emissions of an Ammonia/Diesel Dual-Fuel Engine Using Split-Injection Strategy.” *Fuel* VOL. 378 No. 1 (2024): pp. 128830. DOI: 10.1016/j.fuel.2024.128830.

[52] Zheng, Lei, Mi, Shuang, and Li, Hao. “Experimental Study on the Combustion and Emission Characteristics of Ammonia-Diesel Dual Fuel Engine Under High Ammonia Energy Ratio Conditions.” *Journal of the Energy Institute* VOL. 114 No. 1 (2024): pp. 103–112. DOI: 10.1016/j.joei.2024.01.005.

[53] “TSU 89 70”. British Rail, Derby, United Kingdom. 1989.

[54] “Class 37 Locomotives Static Test - Workshop Overhaul Standard Specification”. 600/19 (WOSS 600/19). British Rail, Derby, United Kingdom. 1990 and 1991.

[55] “Rail Industry Standard RIS-2472-RST.” Data Recorders on Trains. RSSB, London, United Kingdom. 2021.